

The Relative Lens-Source Proper Motion in MACHO 98-SMC-1

M. D. Albrow¹, J.-P. Beaulieu², J. A. R. Caldwell³, D. L. DePoy⁴, M. Dominik², B.
S. Gaudi⁴, A. Gould⁴, J. Greenhill⁵, K. Hill⁵,
S. Kane^{5,6}, R. Martin⁷, J. Menzies³, R. M. Naber², K. R. Pollard¹,
P. D. Sackett², K. C. Sahu⁶, P. Vermaak³, R. Watson⁵, A. Williams⁷

The PLANET Collaboration

and

R. W. Pogge⁴

ABSTRACT

We present photometric and spectroscopic data for the second microlensing event seen toward the Small Magellanic Cloud (SMC), MACHO-98-SMC-1. The lens is a binary. We resolve the caustic crossing and find that the source took $2\Delta t = 8.5$ hours to transit the caustic. We measure the source temperature $T_{\text{eff}} = 8000$ K both spectroscopically and from the color $(V - I)_0 \sim 0.22$. We find two acceptable binary-lens models. In the first, the source crosses the caustic at $\phi = 43^\circ.2$ and the unmagnified source magnitude is $I_s = 22.15$. The angle implies that the lens crosses the source radius in time $t_* = \Delta t \sin \phi = 2.92$ hours. The magnitude (together with the temperature) implies that

¹Univ. of Canterbury, Dept. of Physics & Astronomy, Private Bag 4800, Christchurch, New Zealand

²Kapteyn Astronomical Institute, Postbus 800, 9700 AV Groningen, The Netherlands

³South African Astronomical Observatory, P.O. Box 9, Observatory 7935, South Africa

⁴Ohio State University, Department of Astronomy, Columbus, OH 43210, U.S.A.

⁵Univ. of Tasmania, Physics Dept., G.P.O. 252C, Hobart, Tasmania 7001, Australia

⁶Space Telescope Science Institute, 3700 San Martin Drive, Baltimore, MD. 21218 U.S.A.

⁷Perth Observatory, Walnut Road, Bickley, Perth 6076, Australia

the angular radius of the source is $\theta_* = 0.089 \mu\text{as}$. Hence, the proper motion is $\mu = \theta_*/t_* = 1.26 \text{ km s}^{-1} \text{ kpc}^{-1}$. For the second solution, the corresponding parameters are $\phi = 30^\circ.6$, $I_s = 21.81$, $t_* = 2.15$ hours, $\theta_* = 0.104 \mu\text{as}$, $\mu = \theta_*/t_* = 2.00 \text{ km s}^{-1} \text{ kpc}^{-1}$. Both proper-motion estimates are slower than 99.5% of the proper motions expected for halo lenses. Both are consistent with an ordinary binary lens moving at $\sim 75\text{--}120 \text{ km s}^{-1}$ within the SMC itself. We conclude that the lens is most likely in the SMC proper.

Subject headings: astrometry, gravitational lensing, dark matter, galaxies: individual (Small Magellanic Cloud, Large Magellanic Cloud)

1. Introduction

When microlensing searches toward the Large Magellanic Cloud (LMC) were initiated seven years ago, it was believed that the microlensing events themselves could resolve the question of whether the Galactic dark halo is composed primarily of baryonic material in the form of Massive Compact Halo Objects (MACHOs). The major potential difficulty was thought to be the problem of distinguishing lensing events from variable stars.

The situation today differs markedly from these expectations. On the one hand, more than a dozen candidate events have been detected toward the LMC (Aubourg et al. 1993; Alcock et al. 1997a), and while a few may be intrinsic variables, the great majority are clearly due to genuine microlensing events. On the other hand, the interpretation of these events is far from clear. The optical depth is $\tau \sim 2.5 \times 10^{-7}$ (Alcock et al. 1997a), about half what would be expected from a full dark halo of MACHOs, and far more than could be due to known populations of stars along the line of sight in the Galactic disk, Galactic spheroid, and LMC disk. By contrast, from the measured Einstein crossing times $t_E \sim 45$ days and the well-constrained kinematics of the halo, the mass of these objects would appear to be $0.4 M_\odot$. These could not be made of hydrogen or the population would be discovered easily. The paucity of obvious solutions has led to a large number of alternative explanations for the observed events, including stars within the LMC bar/disk (Sahu 1994), a disrupted dwarf galaxy in front of the LMC (Zhao 1998, Zaritsky & Lin 1997), a warped and flared Milky Way disk (Evans et al. 1998), non-standard halo kinematics, and a halo composed of white dwarfs. However, all of these solutions present considerable difficulties (Gould 1995, 1998a; Beaulieu & Sackett 1998; Bennett 1998; Fields, Freese, & Graff 1998; Gyuk & Gates 1998).

More observations of the type already in progress seem unlikely to resolve the issue by themselves; new methods and strategies will be required. One approach is to search for microlensing toward the Small Magellanic Cloud (SMC). If the LMC events are due to halo lenses, these should produce events of similar duration and frequency, though not identical if the halo is significantly flattened (Sackett & Gould 1993). MACHO (Alcock et al. 1997b), EROS (Palanque Delabrouille et al. 1998) and OGLE (Udalski et al. 1998) are carrying out such observations but, since the SMC has many fewer stars (and hence fewer expected events), this strategy is unlikely to resolve the matter by itself within the next few years.

Another approach is intensive photometric monitoring of ongoing events with the aim of measuring either “parallax” or “proper motion.” These measure respectively v/x and $v/(1-x)$ where v is the transverse speed of the lens relative to the observer-source line of sight, and x is the ratio of the lens to source distance, and can distinguish between halo and LMC lenses almost on a case-by-case basis (Boutreux & Gould 1996). Typical events are long enough that the Earth’s motion would often cause detectable “parallax” deviations in the light curves if the lenses were in the halo, provided that all events were monitored intensively for their entire duration (Gould 1998b). GMAN (Alcock et al. 1997c) is currently following all LMC and SMC events with the aim of detecting this effect, although probably with insufficient intensity to do so in most cases. EROS and MACHO have recently jointly proposed much more intensive follow-up observations at the European Southern Observatory, but have not as yet been awarded telescope time. Proper motions can be measured if a lens caustic (region of formally infinite magnification) passes over the face of the source. The finite size of the source suppresses this infinite magnification according to its size. By modeling the light curve, one can therefore measure t_* , the time it takes the lens to cross the source radius. The angular size of the source, θ_* can be estimated from its color, flux and the Planck law. The proper motion is then given by,

$$\mu = \frac{\theta_*}{t_*} \tag{1}$$

Unfortunately, the majority of events are caused by point-mass lenses for which the caustic is a single point. The probability that this point will pass over the face of a typical source is $\lesssim 10^{-2}$. However, for binary lenses of near-equal mass ratio, the caustics are closed curves whose size is of order the Einstein radius. This means that when there is one crossing, there is usually a second – with forewarning.

On 8 June 1998, MACHO (<http://darkstar.astro.washington.edu>) issued an alert for such a second caustic crossing for the second event discovered toward the SMC, MACHO-98-SMC-1 (J2000 $\alpha = 00:45:35.2$, $\delta = -72:52:34$). This alert provided a rare opportunity to determine the lens location for at least one SMC event.

2. Observations

The Probing Lensing Anomalies NETwork (PLANET) was formed to monitor ongoing microlensing events on a round-the-clock basis from observatories girding the southern hemisphere with a view to detecting anomalies in the light curves which might betray the presence of a planetary companion to the lensing object (Albrow et al. 1998). We have obtained substantial dedicated telescope time during the bulge season (southern Autumn and Winter) on the SAAO 1 m (South Africa, $20^{\circ} 49'$, -32°), the CTIO-Yale 1 m (Chile, $289^{\circ} 11'$, -30°), the Canopus 1 m (Tasmania, $147^{\circ} 32'$, -43°), and the Perth 0.6 m (Western Australia, $116^{\circ} 8'$, -32°). In addition, we fortuitously obtained additional observations from the CTIO 0.9 m. All of our previous monitoring was of bulge events because they are the most common and are concentrated in a relatively compact observing season. However, in view of the importance of MACHO-98-SMC-1, we focused a major effort upon it.

Nightly observations (weather permitting) were made from the SAAO 1 m, the CTIO-Yale 1 m, the CTIO 0.9 m, and the Canopus 1 m from 9 June to 17 June. These consisted typically of 5 to 20 min exposures depending on the source brightness, mostly in Cousins I , but with some in Johnson V . Reductions were performed at the telescope as detailed in Albrow et al. (1998). On 15 June, MACHO predicted that the second crossing would occur on 19.2 ± 1.5 June UT on the basis of a binary-lens fit which they put on their web site. From PLANET observations alone (and confirmed with the addition of earlier MACHO observations posted on their Web site) we were able on 17 June to refine the prediction of the peak to be 18.0 June UT and issued our own caustic alert including light-curve data. For the next two days, we devoted all available telescope time to this event, and then continued sparser observations into the beginning of July.

In addition, we obtained a spectrum of the source during the caustic crossing on 18 June when the source was $I \sim 17$ using the 1.9 m SAAO telescope and grating spectrograph at a resolution of about 7\AA .

3. Analysis

The proper motion can be determined using equation (1) from measurements of the source crossing time, t_* , and the angular source radius, θ_* . The crossing time

is extracted from the light curve, while the source radius can be measured by two independent methods, spectroscopic and photometric.

3.1. Measurement of t_*

A static binary lens with a uniform surface-brightness finite source generates a light curve characterized by nine parameters. Three of these are t_E , t_0 , and $u_0 (\geq 0)$, the Einstein radius crossing time, the time of closest approach, and the impact parameter of a hypothetical event in which the binary is replaced by a single point-lens of the same total mass placed at the geometrical midpoint of the binary. Two other parameters are I_s and I_b , the magnitudes of the lensed source and of any unresolved (unlensed) light superposed on the source star, respectively. Three parameters specific to the binary character of the lens are the mass ratio $q = M_2/M_1$ of the secondary to the primary ($0 < q \leq 1$), the projected binary separation d in units of the (combined) Einstein radius r_E , and the angle α ($0 \leq \alpha < 2\pi$) between the binary-separation vector (M_2 to M_1) and the proper motion of the source relative to the binary center of mass (see Fig. 1). The direction of the relative motion between lens and source is chosen so that the lens system is on the right hand side of the moving source. Finally, $\rho_* \equiv \theta_*/\theta_E$ is the source radius in units of the angular Einstein radius.

Once the full solution is found, the crossing time is given by $t_* = \rho_* t_E$. In order to understand the sources of uncertainty in this determination, however, it is useful to write the equation as,

$$t_* = \Delta t \sin \phi, \quad \Delta t \equiv \rho_* t_E \csc \phi, \quad (2)$$

where ϕ is the angle at which the source crosses the caustic (see inset to Fig. 1). The quantity $(2\Delta t)$ is the time taken by the source to transit the caustic. If the caustic crossing is well monitored (as it is in this case) then Δt is determined to high precision. We find below that $\Delta t = 4.25$ hours. Most of the uncertainty in t_* therefore comes from the angle ϕ , which is determined from the *global* fit of the light curve. If the data permit two or more discrete geometries, then $\sin \phi$ can take on substantially different values.

Figure 2 shows data (nightly binned except at the peak) together with the light curves for our models I and II. Figure 1 shows the lens geometry, the resulting

caustic structure, and the trajectory of the source relative to this structure for model I, which has parameters $t_E = 108.4$ days, $t_0 = 27.83$ May 1998 UT, $u_0 = 0.065$, $I_s = 22.15$, $I_b = 21.43$, $\alpha = 348^\circ.2$, $q = 0.29$, $d = 0.59$, and $\rho_* = 0.00112$. In particular, $t_* = \rho_* t_E = 2.92$ hours. The source center passed over the caustic at UT 18.120 June. The overall fit has $\chi^2 = 394$ for 164 degrees of freedom. The model II parameters are $t_E = 80.3$ days, $t_0 = 10.68$ June 1998 UT, $u_0 = 0.036$, $I_s = 21.81$, $I_b = 21.89$, $\alpha = 351^\circ.4$, $q = 0.95$, $d = 0.56$, and $\rho_* = 0.00112$, with $t_* = 2.15$ hours, and $\chi^2 = 442$. Note that the values of t_* are quite different in the two models despite the fact that values of Δt (4.26 hours and 4.23 hours) are very similar. The difference is due to the different angles at which the source crosses the caustic, $\phi = 43^\circ.2$ and $30^\circ.6$ respectively. The differences in t_* and I_s lead to a proper motion that is larger for model II by a factor of 1.59. The model II χ^2 is ~ 48 higher than for model I. However, the fact that model I has a better fit does not rule out model II, which gives an acceptable fit to the data. Hence, the difference in proper motions between the two models (which is much larger than the statistical error of each solution) gives a good indication of the systematic uncertainty. It is possible that this uncertainty will be removed as we acquire more data, or by combining our data set with those of MACHO and EROS. In particular, we note that model I appears more consistent with the pre-first-caustic data that MACHO put on their web site. However, at present we must allow that our proper motion could be off by a factor ~ 1.6 .

We have also fit for V_s and V_b holding all seven other parameters fixed at the values found for the I band solutions. For model I, we find $[V, (V - I)] = (22.45, 0.3)$, $(21.75, 0.3)$, and $(21.30, 0.3)$ for the source, background, and total light respectively. For model II, we find $(22.10, 0.3)$, $(21.80, -0.1)$, and $(21.20, 0.1)$. Initially, the MACHO web page estimated the total baseline values to be $V = 21.8$, $V - R = 0.1$. After the appearance of this *Letter* as a preprint, MACHO (A. Becker 1998 private communication) informed us that they had revised their estimate to $V = 21.4$. In addition, OGLE (A. Udalski 1998 private communication) confirmed this value, finding $V = 21.41 \pm 0.23$. Since our fits contain no data from the baseline, these independent measurements of the baseline flux serve as an important check on the viability of the models.

Our determinations may be compared with those of the EROS collaboration (Afonso et al. 1998) based on a single night of data covering the end of the caustic crossing. They found a lower limit $\Delta t > 3$ hours and measured the end of the caustic

crossing at UT 7:08 \pm 0:02 18 June 1998. In our model I, $\Delta t = 4.26$ hours, and the end of the caustic crossing is at UT 7:11 18 June 1998.

3.2. Measurement of θ_*

We estimate the angular radius of the source, θ_* , from the light curve. The model I fit to the overall light curve yields an unlensed source magnitude $I = 22.15$. We determine the color of the source, $V - I = 0.31 \pm 0.02$, from its measured color near the caustic, transforming our instrumental magnitudes to standard Johnson/Cousins bands using a sample of stars in our data set that were independently calibrated by OGLE (Udalski et al. 1998). Note that while the color of the source at any particular time on the light curve could be affected by blending, this effect is extremely small near the caustic because the source is magnified by a factor ~ 100 . We assume an extinction $A_V = 0.22 \pm 0.1$ (see below). This implies $I_0 = 22.02$ and $(V - I)_0 = 0.22$. At fixed $(V - I)_0$ color, the effective temperature depends only very weakly on metallicity (which we take to be $[\text{Fe}/\text{H}] = -0.75$). We use the Yale Isochrones (Green, Demarque, & King 1987) to estimate $T_{\text{eff}} \sim 7900 \pm 300$ K. Combining this with the dereddened flux, and again using the Yale Isochrones, we find $\theta_* = 0.089 \mu\text{as}$.

We now investigate the effects of various errors. First an extinction error of δA_V , alters I_0 by $-\delta A_I \sim -0.6\delta A_V$ (Stanek 1996), leading to an incorrect estimate of the radius by $(\delta\theta_*/\theta_*) \sim (\ln 10/5)0.6\delta A_V$. This would be more than compensated, however, by the fact that the color would be in error by $\delta E(V - I) \sim 0.4\delta A_V$. This in turn would lead to an incorrect estimate of the temperature and so of the I band surface brightness, $\delta(2.5 \log S) \sim \gamma\delta E(V - I)$, where $\gamma \equiv [(\partial \ln B_V / \partial T) / (\partial \ln B_I / \partial T) - 1]^{-1}$, and B_V and B_I are the Planck intensities at $0.55 \mu\text{m}$ and $0.80 \mu\text{m}$, respectively. This causes an error in the radius of $(\delta\theta_*/\theta_*) \sim -(\ln 10/5)0.4\gamma\delta A_V$. Thus, the net error is $(\delta\theta_*/\theta_*) \sim (\ln 10/5)(0.6 - 0.4\gamma)\delta A_V \sim -0.25\delta A_V$, for $T \sim 8000$ K.

By interpolating the extinction map of Schlegel, Finkbeiner, & Davis (1988) across the SMC, we find a foreground extinction of $A_V = 0.12$. We adopt an internal extinction of 0.1 ± 0.1 mag, and obtain $A_V = 0.22 \pm 0.1$. From the discussion above, the extinction uncertainty yields an uncertainty in the radius of $\sim 3\%$. The 300 K uncertainty in the temperature, which arises primarily from the uncertain color

calibration of the models (M. Pinsonneault 1998 private communication) generates a 5% uncertainty in the radius. Finally, the $\sim 10\%$ uncertainty in the unmagnified flux of the source produces another 5% uncertainty in the radius, for a final estimate of $\theta_* = 0.089 \pm 0.007 \mu\text{as}$.

From the spectrum, we find that the source temperature is consistent with the value $T = 8000$ K that was estimated from the color $(V - I)_0 \sim 0.22$, i.e., roughly an A6 star. The flux ($V_0 = 22.24$) is in reasonable agreement with what one would expect from a metal-poor star at 8000 K ($M_V \sim 3.2$) at the distance of the SMC (~ 60 kpc.) Figure 3 shows the source spectrum.

4. Results

Combining the measurements of θ_* and t_* we find

$$\mu = \frac{\theta_*}{t_*} = 1.26 \pm 0.10 \text{ km s}^{-1} \text{ kpc}^{-1}, \quad (3)$$

for model I, where we have assumed that the error in t_* is much smaller than in θ_* . As noted in the previous section however, model II yields $\mu = 2.00 \text{ km s}^{-1} \text{ kpc}$. Hence, the difference between acceptable solutions is much larger than the error in each solution. Figure 4 shows the distribution of proper motions expected from a standard $\rho_*(r) \propto r^{-2}$ isothermal halo characterized by a rotation speed $v_c = 220 \text{ km s}^{-1}$, and assuming an SMC distance of 60 kpc (Barnes, Moffett, & Gieren 1993). Since the proper motion of the SMC is difficult to measure and not yet tightly constrained (e.g. Kroupa & Bastian 1997), we show curves for 4 separate assumptions: three with an SMC transverse speed of 250 km s^{-1} oriented at 0° , 90° , and 180° relative to the reflex motion of the Sun, and the fourth with no transverse speed. In all four cases we find that the fraction of events with proper motions smaller than that given by equation (3) is less than 0.1% for model I. For model II the fraction is less than 0.5%. This would seem to imply that the lens is not in the halo.

The main alternative explanation for the event is that the lens is in the SMC. In this case, its transverse speed relative to the source is $v \sim 75 \text{ km s}^{-1}$ for model I and $v \sim 120 \text{ km s}^{-1}$ for model II. The measured one-dimensional dispersion of the SMC carbon stars is $\sigma \sim 21 \pm 2 \text{ km s}^{-1}$ (Hatzidimitriou et al. 1997). Figure 4 shows the expected distribution of proper motions assuming that both the lens and the

source transverse velocity distributions are characterized by this speed. That is, the SMC material is assumed to be characterized by a single component (but see below). The fraction of all events with proper motions $\mu > 1.26 \text{ km s}^{-1} \text{ kpc}^{-1}$ is $\sim 9\%$. The fraction with $\mu > 2.00 \text{ km s}^{-1} \text{ kpc}^{-1}$ is $< 0.1\%$.

Another possibility is that we are seeing material that has been tidally disrupted and is moving transversely at $75\text{--}120 \text{ km s}^{-1}$. There is substantial evidence for such rapidly moving material in *radial velocity* studies of the SMC. The extensive HI observations of McGee & Newton (1981) show that the SMC has four principal and overlapping structures at velocities $v_h = 114, 133, 167$ and 192 km s^{-1} . McGee & Newton (1981) state that of the 506 lines of sight examined, 97% show evidence for multiple peaks. Staveley-Smith et al. (1997) present much more detailed HI maps and argue that these data imply not multiple components but rather a complexly structured and perhaps disintegrating SMC. Zhao (1998) has modeled the SMC as comoving tidal debris and predicted that such a structure should generate about one microlensing event per year. Torres & Carranza (1987) summarize evidence for 4 peaks at $v_h = 105, 140, 170,$ and 190 km s^{-1} from their own HII data plus earlier results for HI, planetary nebulae, supergiants, emission regions, and CaII. However, the picture that they present is much more of correlations between radial velocity and position on the sky. Of course, to produce the observed proper motion, there must be material at two different velocities along the same line of sight. We therefore believe that it is plausible, but by no means proven, that there is material within the SMC that could produce the proper motion indicated by model II. (As discussed above, the proper motion associated with model I can be explained from the internal dispersion of clumps within the SMC alone.)

If the lens does lie in the SMC, then the Einstein radius is approximately $r_E \sim (4GM D_{\text{LS}}/c^2)^{1/2}$, where D_{LS} is the lens-source separation. The observed time scale is $t_E = r_E/v = 108$ days or 82 days for the two solutions. Hence, the mass is

$$M \sim \frac{v^2 t_E^2 c^2}{4G D_{\text{LS}}} \sim 0.53 M_{\odot} \left(\frac{D_{\text{LS}}}{5 \text{ kpc}} \right)^{-1}, \quad (4)$$

for model I and a factor 1.4 times larger for model II. Various studies have found that the SMC is extended along the line of sight. Although the original estimates of 20 kpc or more by Mathewson, Ford, & Visvanathan (1986) are probably too high, the depth may be as high as 10 kpc (Welch et al. 1987; Martin, Maurice, & Lequeux 1989; Hatzidimitriou, Cannon, & Hawkins 1993). Equation (4) implies that if the lens-source separation is comparable to this depth, then the total mass of the

lens is that of a typical low-mass binary. The projected separation of the binary is $dr_E = bvt_E \sim 2.7$ AU or $dr_E \sim 3.1$ AU, which are also quite reasonable for a low-mass binary. The period would then be $P \sim 6(D_{LS}/5 \text{ kpc})^{1/2}$ years, indicating that the effect of internal binary motion during the event is small.

In sum, MACHO-98-SMC-1 appears to be consistent with lensing by a stellar binary in the SMC proper, and inconsistent with lensing by an object in the Galactic halo.

We thank the SAAO, CTIO, Canopus and Perth Observatories for generous awards of time to PLANET science. We thank David Gonzalez, Juan Espinoza, and Charles Bailyn who obtained much of the CTIO-Yale 1 m data. We thank Philip Keenan and Arne Sletteback for valuable discussion about the spectral type of the source. We thank B. Atwood, T. O'Brien, P. Byard, and the entire staff of the OSU astronomical instrumentation lab for building the instrument used at the CTIO-Yale 1-m telescope. We give special thanks to the MACHO collaboration for making the public alerts of this event and its probable impending second caustic crossing, which made possible the observations reported here. This work was supported by grants AST 97-27520 and AST 95-30619 from the NSF, by grant NAG5-7589 from NASA, by a grant from the Dutch ASTRON foundation, and by a Marie Curie Fellowship from the European Union.

REFERENCES

- Afonso, C. et al. 1998, *A&A*, 337, L17
- Albrow, M. et al. 1998, *ApJ*, 509, 000
- Alcock, C. et al. 1997a, *ApJ*, 486, 697
- Alcock, C. et al. 1997b, *ApJ*, 491, L11
- Alcock, C. et al. 1997c, *ApJ*, 491, 436
- Aubourg, E., et al. 1993, *Nature*, 365, 623
- Barnes, T.G., Moffett, T.J., & Gieren, W.P. 1993, *ApJ*, 405, L51
- Beaulieu, J.-P., & Sackett, P. D. 1998, *AJ*, 116, 209
- Bennett, D. 1998, *ApJ*, 493, L79
- Boutreux, T., & Gould, A. 1996, *ApJ*, 462, 705
- Evans, N. W., Gyuk, G., Turner, M. S., & Binney, J. J. 1998, *ApJ*, 501, L29
- Fields, B.D., Freese, K., Graff, D.S. 1998, *New Astronomy*, 3, 347
- Gould, A. 1995, *ApJ*, 441, 77
- Gould, A. 1998a, *ApJ*, 499, 728
- Gould, A. 1998b, *ApJ*, 506, 000
- Green, E. M., Demarque, P., & King, C. R. 1987, *The Revised Yale Isochrones and Luminosity Functions* (New Haven: Yale Univ. Observatory)
- Gyuk, G., & Gates, E. 1998 *MNRAS*, 294, 682
- Hatzidimitriou, D., Croke, B.F., Morgan, D.H., & Cannon, R.D. 1997, *A&AS*, 122, 507
- Kroupa, P., & Bastian, U. 1997, *New Astronomy*, 2, 77
- Martin, N., Maurice, E., & Lequeux, J. 1989, *A&A*, 215, 219
- Mathewson, D.S., Ford, V.L., & Visvanathan, N., 1986, *ApJ*, 301, 664
- McGee, R.X., & Newton, L.M. 1981, *Proc. ASA*, 4, 189
- Palanque-Delabrouille, N. et al. 1998, *A&A*, 332, 1
- Sackett, P. D. & Gould, A. 1993, *ApJ*, 419, 648
- Sahu, K. C. 1994, *Nature*, 370, 275

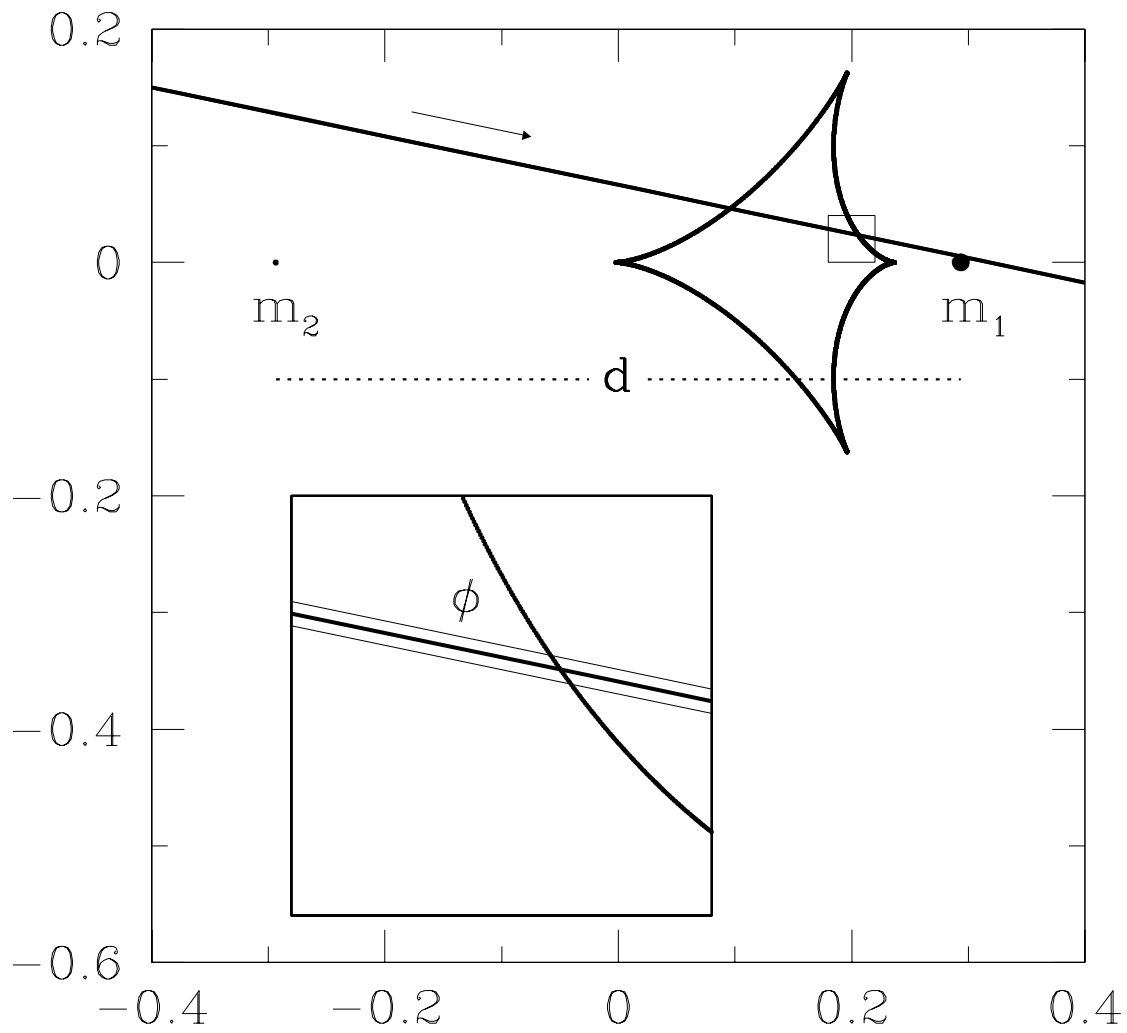
- Schlegel, D., Finkbeiner, & Davis, M. 1998, *ApJ*, 500, 525
- Stanek, K. Z. 1996, *ApJ*, 460, L37
- Staveley-Smith, L., Sault, R.J., Hatzidimitriou, D., Kesteven, M.J., & McConnell, D., 1997, *MNRAS*, 289, 225
- Torres, G., & Carranza, G.J., 1987, *MNRAS*, 226, 513
- Udalski, A., Szymański, M., Kubiak, M., Pietrzyński, G., Woźniak, P., & Żebruń, K. 1998, *AcA*, 48, 147
- Welch, D.L., McLaren, R.A., Madore, B.F., & McAlary, C.W. 1987, *ApJ*, 321, 162
- Zaritsky, D., & Lin, D. N. C. 1997, *AJ*, 114, 2545
- Zhao, H. 1998, *MNRAS*, 294, 139

Fig. 1.— Geometry of model I. The diamond shaped curve is the caustic, i.e., the region of formally infinite magnification. The thick solid line and two thinner parallel lines indicate the source trajectory and the finite size of the source. The tick marks are in units of the Einstein radius crossing time, $t_E = 108.4$ days. The two components of the binary are shown by *circles* whose relative sizes are proportional to their masses. Their projected separation in units of the Einstein ring is labeled d . The insert shows more clearly the finite size of the source as well as the angle ϕ at which the source intercepts the caustic.

Fig. 2.— Light curve of the PLANET data for MACHO-98-SMC-1. Shown are the data from the SAAO 1 m (*circles*), the CTIO 0.9 m (*squares*), the CTIO-Yale 1 m (*triangles*), and the Canopus 1 m (*asterisks*). The inset covers about 0.6 days, corresponding to less than one tick mark on the main figure. The data are binned by day (except near the caustic) for clarity. The light-curve fits were done without binning. The two curves show model I (*bold*) and model II (*solid*). The two models have very similar crossing times, $\Delta t \sim 4.25$ hours (which are determined from the caustic crossing), but different angles at which the lens crosses the caustic (see Fig 1), $\phi = 43^\circ.2$ versus $\phi = 30^\circ.6$ (which are determined from the overall light curve). The proper motion is determined from the combination $\mu = \theta_*/t_* = \theta_*/(\Delta t \sin \phi)$ where θ_* is the angular size of the source.

Fig. 3.— PLANET spectrum of MACHO-SMC-98-1 taken near 18.0 June 1998 UT. The obvious Balmer line absorption indicates the source is an A-type star, consistent with the spectral type estimated from the $V - I$ color of the source. The strength of weak CaII H and K absorption suggests the effective temperature of the star is close to 8000K, although the Balmer line absorption strengths seem to indicate a slightly higher temperature. Note that the spectrograph slit was not well aligned with the parallactic angle, so the overall spectral energy distribution may be affected.

Fig. 4.— Distribution of expected proper motions from Galactic halo (right) and non-tidal SMC (left) lenses. The SMC model is based on a one-dimensional dispersion of 21 km s^{-1} for both the lenses and sources. The normalizations are set arbitrarily to unity at the peaks. Four models are shown for the halo, three where the SMC is moving transversely at 250 km s^{-1} at 0° (*solid*), 90° (*dashed*), and 180° (*bold dashed*) relative to the reflex motion of the Sun, and one where the SMC has no transverse motion (*bold*). The boxes shows the best fit and 1σ errors for the proper motion of the lens for model I (left) and model II (right). The central values lies below 99.9% (99.5%) of the halo distribution and above 91% (99.9%) of the SMC distribution. The observed value is inconsistent with the halo hypothesis. The lens and source could possess normal SMC kinematics or one of them could be part of SMC tidal debris.



Days Since UT 31.0 May

